

# Thermodynamic Bethe Ansatz for boundary sine-Gordon model

Taejun Lee and Chaiho Rim

*Department of Physics, Chonbuk National University  
 Chonju 561-756, Korea  
 email: tjun@pine.chonbuk.ac.kr, rim@mail.chonbuk.ac.kr*

## Abstract

(R-channel) TBA is elaborated to find the effective central charge dependence on the boundary parameters for the massless boundary sine-Gordon model with the coupling constant  $(8\pi)/\beta^2 = 1 + \lambda$  with  $\lambda$  a positive integer. Numerical analysis of the massless boundary TBA demonstrates that at an appropriate boundary parameter range (cusp point) there exists a singularity crossing phenomena and this effect should be included in TBA to have the right behavior of the effective central charge.

## 1 Introduction

The low dimensional quantum system such as a quantum wire with boundaries is not easy to study in terms of mean field approach due to large quantum fluctuations. The system is also strongly affected by the the existence of boundaries. For example, one needs a good knowledge of the the low dimensional quantum field theory to study the quantum Hall edge tunnelling [1] .

In this work, the massless Tomonaga-Luttinger liquid with boundaries is studied motivated by SNS junction super-conductor analysis[2, 3]. This system is summarized in terms of the boundary sine-Gordon model(bSG).

$$\mathcal{A} = \int d^2x \frac{1}{4\pi} (\partial_a \varphi)^2 - \mu_B^{(1)} \int_{y=0} dx 2 \cos(b(\varphi - \varphi_0^{(1)})) - \mu_B^{(2)} \int_{y=R} dx 2 \cos(b(\varphi - \varphi_0^{(2)})) . \quad (1-1)$$

The free energy dependence of the finite system on the boundary parameter  $\chi = b(\varphi_0^{(2)} - \varphi_0^{(1)})$  is one of the demanding questions. To do this, we first consider the massive sine-Gordon model with boundaries and put the bulk mass vanish [4].

The massive bSG is written as

$$\mathcal{A} = \int d^2x \left[ \frac{1}{4\pi} (\partial_a \varphi)^2 - 2\mu (\cos(2b\varphi) - 1) \right] - \mu_B^{(1)} \int_{y=0} dx 2 \cos(b(\varphi - \varphi_0^{(1)})) - \mu_B^{(2)} \int_{y=R} dx 2 \cos(b(\varphi - \varphi_0^{(2)})), \quad (1-2)$$

The coupling constant  $b^2$  is restricted to be less than 1. (Note that  $b^2$  is scaled by  $8\pi$  from the conventional choice  $\beta^2 = 8\pi b^2$ ).

The bulk sine-Gordon model (SG) [5] belongs to the category of two dimensional integrable quantum field theories and allows an exact treatment of the system. Integrable quantum systems have been studied systematically after the pioneering work of Zamolodchikov [6]. The integrability of the bSG was also demonstrated in [7].

The scale dependence of the system can be studied by the method of thermodynamic Bethe ansatz (TBA) [8, 9]. Suppose a system lies along the  $y$ -axis with a finite size  $R$  and appropriate boundary conditions are imposed at each end as in Fig (1). The  $x$ -direction is periodic and its size  $L$  is put to  $\infty$  in the thermodynamic limit.

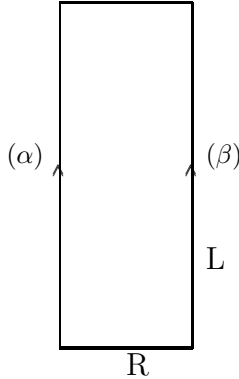


Figure 1: space with two boundaries: boundary condition  $(\alpha)$  and boundary condition  $(\beta)$ .

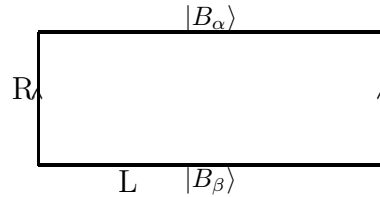


Figure 2: space with states: initial states  $|B_\alpha\rangle$  and final state  $|B_\beta\rangle$ .

The partition function with these boundaries is given as

$$Z_{\alpha\beta} = \text{Tr} e^{-LH_{\alpha\beta}} \cong e^{-LE_{\alpha\beta}(R)}$$

for large  $L$ .  $H_{\alpha\beta}$  is the Hamiltonian of the system of size  $R$  with boundary  $(\alpha)$  and  $(\beta)$ .  $E_{\alpha\beta}(R)$  is the ground state energy in the thermodynamic limit, which depends on the size  $R$ .

The same system can be viewed as the one with initial state  $|B_\beta\rangle$  and final state  $|B_\alpha\rangle$ . In this picture, the bulk is periodic in  $L$  as in Fig. (2). Then the same partition function is evaluated using the periodic Hamiltonian  $H$  of the system.

$$Z_{\alpha\beta} \equiv e^{-RLf_{\alpha\beta}(R)} = \langle B_\alpha | e^{-RH} | B_\beta \rangle = \left( \sum_{\{A\}} \frac{\langle B_\alpha | A \rangle \langle A | B_\beta \rangle e^{-RE_A}}{\langle A | A \rangle} \right), \quad (1-3)$$

where  $f_{\alpha\beta}(R)$  is the free energy density per length and  $\{A\}$  is the complete set of the periodic Hamiltonian eigenstates. The finite size effect of the SG (with boundary) was analyzed in [4, 10] for diagonal case using thermodynamic Bethe ansatz (R-channel TBA).

In section 2, we present the massive (R-channel) TBA for the bulk sine-Gordon model with boundary sine-Gordon interaction. In this analysis, we restrict the coupling constant  $\lambda = 1/b^2 - 1 \equiv n_b + 1$  to a positive integer ( $n_b \geq 0$ ) so that the bulk scattering matrix is diagonal but non-diagonal boundary scattering is allowed. The topological charge violation at the boundary is incorporated following the suggestion given in [2]. This TBA has the bulk and boundary scale dependence as well as the boundary parameter dependence.

In section 3, (R-channel) TBA for the massless boundary sine-Gordon model is obtained as the massless limit of the massive TBA. It is demonstrated through numerical work that beyond a certain parameter range ( $\chi \geq b^2\pi$ ), a branch singularity crossing occurs. Thus the original ground state TBA which holds within a small parameter range is to be modified. We investigate on the singularity structure of TBA and find that only one singularity of each species is moving on the complex plane. This has the effect on the evaluation of the convolution in TBA. From this branch singularity crossing information, we propose a modified massless TBA according to the suggestion in [2, 11, 12, 13] similarly in the bulk case [14]. Section 4 is the conclusion.

## 2 Massive TBA for boundary sine-Gordon

The bulk sine-Gordon periodic potential allows a soliton with topological charge +1 and an antisoliton with the charge -1. Both of them have the same mass  $M$  as the result of the charge conjugation symmetry,  $\phi \rightarrow -\phi$ . The mass is given in terms of  $\mu$  [15],

$$\frac{\pi\mu}{\gamma(b^2)} = \left[ M \frac{\sqrt{\pi}}{2} \frac{\Gamma(\frac{1}{2-2b^2})}{\Gamma(\frac{b^2}{2-2b^2})} \right]^{2-2b^2} \quad (2-1)$$

In addition, there are topologically neutral particles, breathers (interpreted as the soliton-antisoliton bound states). Their masses are given as

$$M_a = Mm_a = 2M \sin\left(\frac{\pi a}{2\lambda}\right) \quad a = 1, 2, \dots, n_b. \quad (2-2)$$

$n_b$  is the number of breather species,  $n_b =$  positive integer less than  $\lambda$ .

The free energy density in Eq. (1-3) is expanded in terms of the bulk Hamiltonian eigenstates, *i.e.*, solitons, antisolitons and breathers. These states are uniquely identified in terms of mass and rapidity due to the Fermi-statistics.

The presence of the boundary forces two restrictions on the states. First, the pair creation at the boundary forces the rapidity paired ( $\theta, -\theta$ ) and therefore, one can count  $\theta$  positive and make energy eigenvalue doubled:  $E_A(\theta) = 2M_A \cosh \theta$  where  $M_A$  is the single particle mass.

Second, at the boundary an in-coming soliton is allowed to be scattered away as an antisoliton and vice versa since the soliton number is not conserved in general. To take



Figure 3: pair creation at the boundary

care of this, soliton and antisoliton are regarded as a constituent of a doublet of identical particles [2]. When the partition function in Eq. (1-3) is written in terms of spectral density  $\rho$ ,  $Z_{\alpha\beta} = \int [d\rho] \exp(-RL f_{\alpha\beta}(L, R))$ , the spectral density should include not only one-particle density of topological particle (denoted as  $\rho_0$ ) (soliton is indistinguishable from antisoliton) and its hole density ( $\rho_{h0}$ ), one-particle density of a breather ( $\rho_a$ ), its hole density ( $\rho_{ha}$  with  $1 \leq a \leq n_b$ ) but also should include two-particle density of topological particles ( $\rho_d$ ) (*i.e.* soliton and antisoliton pair). The densities are summarized in the Table 1:

species	density
soliton or/and antisoliton	$\rho_0, \rho_d, \rho_{h0}$
breather	$\rho_a, \rho_{ha}, \quad a = 1, \dots, n_b$

Table 1: particle species and the corresponding densities.

Then the free energy density can be written as

$$Rf_{\alpha\beta}(R) = \int_0^\infty d\theta \left\{ \sum_{A=0,1,\dots,n_b} \rho_A (2M_A \cosh \theta - \ln \lambda_{\alpha\beta}^A(\theta)) + \rho_d (2M_d \cosh \theta - \ln \lambda_{\alpha\beta}^d) - \mathcal{S}_B \right\}, \quad (2-3)$$

where  $M_0 = M$  and  $M_d = 2M$ .  $\mathcal{S}_B$  is the entropy density,

$$\begin{aligned} \mathcal{S}_B &= \int_0^\infty d\theta [(\rho_0 + \rho_d + \rho_{h0}) \ln(\rho_0 + \rho_d + \rho_{h0}) - \rho_0 \ln \rho_0 - \rho_d \ln \rho_d - \rho_{h0} \ln \rho_{h0} \\ &\quad + \sum_{a=1,\dots,n_b} \{(\rho_a + \rho_{ha}) \ln(\rho_a + \rho_{ha}) - \rho_a \ln \rho_a - \rho_{ha} \ln \rho_{ha}\}]. \end{aligned} \quad (2-4)$$

$\lambda_{\alpha\beta}^A(\theta) = \langle B_\alpha | \theta A \rangle \langle \theta A | B_\beta \rangle$  is the boundary state contribution, which is given in terms of the boundary scattering amplitude  $R(u)$  with  $u = -i\theta$ :

$$\begin{aligned} \lambda_{\alpha\beta}^a &= \overline{K_\alpha^a(u)} K_\beta^b(u) \quad \text{for } a = 1, 2, \dots, n \\ \lambda_{\alpha\beta}^0 &= \overline{K_\alpha^{++} K_\beta^{++}} + \overline{K_\alpha^{+-} K_\beta^{+-}} + \overline{K_\alpha^{-+} K_\beta^{-+}} + \overline{K_\alpha^{--} K_\beta^{--}} = \text{Tr}(\overline{K_\alpha} K_\beta) \\ \lambda_{\alpha\beta}^d &= (\overline{K_\alpha^{++} K_\alpha^{--}} - \overline{K_\alpha^{+-} K_\alpha^{-+}})(K_\beta^{++} K_\beta^{--} - K_\beta^{+-} K_\beta^{-+}) = \text{Det}(\overline{K_\alpha} K_\beta) \end{aligned} \quad (2-5)$$

where  $K(u) \equiv R(\pi/2 - u)$ .

The boundary scattering amplitude (modulo CDD-type factors), can be found in [7], which satisfies the boundary version of the Yang Baxter equation, unitarity condition, and analyticity-crossing symmetry.

$$R(\eta, \vartheta, u) = \begin{pmatrix} R^{++}(\eta, \vartheta, u) & R^{+-}(\eta, \vartheta, u) \\ R^{-+}Q(\eta, \vartheta, u) & R^{--}(\eta, \vartheta, u) \end{pmatrix}$$

$$\begin{aligned}
&= \begin{pmatrix} P_0^+(\eta, \vartheta, u) & Q_0(u) \\ Q_0(u) & P_0^-(\eta, \vartheta, u) \end{pmatrix} R_0(u) \frac{\sigma(\eta, u) \sigma(i\vartheta, u)}{\cos(\eta) \cosh(\vartheta)}, \\
P_0^\pm(\eta, \vartheta, u) &= \cos(\lambda u) \cos(\eta) \cosh(\vartheta) \mp \sin(\lambda u) \sin(\eta) \sinh(\vartheta) \\
Q_0(u) &= -\sin(\lambda u) \cos(\lambda u).
\end{aligned} \tag{2-6}$$

Here  $R_0$  is the boundary condition independent part,

$$R_0(u) = \prod_{l=1}^{\infty} \left[ \frac{\Gamma(4l\lambda - \frac{2\lambda u}{\pi}) \Gamma(4\lambda(l-1) + 1 - \frac{2\lambda u}{\pi})}{\Gamma((4l-3)\lambda - \frac{2\lambda u}{\pi}) \Gamma((4l-1)\lambda + 1 - \frac{2\lambda u}{\pi})} / (u \rightarrow -u) \right]$$

and  $\sigma(x, u)$  is the boundary condition dependence part,

$$\sigma(x, u) = \frac{\cos x}{\cos(x + \lambda u)} \prod_{l=1}^{\infty} \left[ \frac{\Gamma(\frac{1}{2} + \frac{x}{\pi} + (2l-1)\lambda - \frac{\lambda u}{\pi}) \Gamma(\frac{1}{2} - \frac{x}{\pi} + (2l-1)\lambda - \frac{\lambda u}{\pi})}{\Gamma(\frac{1}{2} - \frac{x}{\pi} + (2l-2)\lambda - \frac{\lambda u}{\pi}) \Gamma(\frac{1}{2} + \frac{x}{\pi} + 2l\lambda - \frac{\lambda u}{\pi})} / (u \rightarrow -u) \right].$$

The scattering parameters,  $\eta$  and  $\vartheta$  are related with the action parameters,  $\mu_B$  and  $\varphi_0$  [16, 17]:

$$\begin{aligned}
\cos(b^2\eta) \cosh(b^2\vartheta) &= \mu_B \sqrt{\sin(b^2\pi)} \cos(b\varphi_0) / \sqrt{\mu} \\
\sin(b^2\eta) \sinh(b^2\vartheta) &= \mu_B \sqrt{\sin(b^2\pi)} \sin(b\varphi_0) / \sqrt{\mu}
\end{aligned} \tag{2-7}$$

The boundary scattering amplitude of breathers is given as

$$R_0^{(k)}(\eta, \vartheta, u) = R_0^{(k)}(u) Z^{(k)}(\eta, u) Z^{(k)}(i\vartheta, u), \quad 1 \leq k \leq n_b. \tag{2-8}$$

$R_0^{(k)}$  is the boundary independent part and  $Z^{(k)}$  the boundary dependent one:

$$R_0^{(k)}(u) = \frac{\left(\frac{1}{2}\right) \left(\frac{k}{2\lambda} + 1\right)}{\left(\frac{k}{2\lambda} + \frac{3}{2}\right)} \prod_{l=1}^{k-1} \frac{\left(\frac{l}{2\lambda}\right) \left(\frac{l}{2\lambda} + 1\right)}{\left(\frac{l}{2\lambda} + \frac{3}{2}\right)^2}, \quad Z^{(k)}(x, u) = \prod_{l=0}^{k-1} \frac{\left(\frac{x}{\lambda\pi} - \frac{1}{2} + \frac{k-2l-1}{2\lambda}\right)}{\left(\frac{x}{\lambda\pi} + \frac{1}{2} + \frac{k-2l-1}{2\lambda}\right)},$$

where the notation  $(x)$  stands for

$$(x) = \frac{\sin\left(\frac{u}{2} + \frac{x\pi}{2}\right)}{\sin\left(\frac{u}{2} - \frac{x\pi}{2}\right)}.$$

The hole and the particle densities are not independent each other. This relation is obtained from the bulk scattering amplitude. The bulk-scattering amplitude of solitons and antisolitons [5] are given as

$$\begin{aligned}
S_{++}^{++}(u) &= S_{--}^{--}(u) = s(u) \\
S_{+-}^{+-}(u) &= S_{-+}^{-+}(u) = \frac{\sin(\lambda u)}{\sin(\lambda(\pi - u))} s(u) \\
S_{+-}^{+}(u) &= S_{-+}^{-}(u) = \frac{\sin(\lambda\pi)}{\sin(\lambda(\pi - u))} s(u)
\end{aligned} \tag{2-9}$$

where  $s(u)$  is given as

$$s(u) = \prod_{l=1}^{\infty} \left[ \frac{\Gamma(2(l-1)\lambda - \frac{\lambda u}{\pi})\Gamma(2l\lambda + 1 - \frac{\lambda u}{\pi})}{\Gamma((2l-1)\lambda - \frac{\lambda u}{\pi})\Gamma((2l-1)\lambda + 1 - \frac{\lambda u}{\pi})} / (u \rightarrow -u) \right]$$

Due to the restriction of  $\lambda$ , the bulk scattering amplitudes are diagonal,  $S_{+-}^{\pm}(u) = 0$ . This restriction makes our analysis not too much complicated [20]. The diagonal scattering amplitude for soliton and antisoliton turns out to be equal up to a phase difference:  $S_{++}^{++}(u) = (-1)^{\lambda-1} S_{+-}^{+-}(u)$ .

The scattering amplitude of the breathers  $B^a$  and  $B^b$  with  $b \leq a \leq n_b$  takes the form

$$S^{ab}(u) = \{a+b-1\}\{a+b-3\}\dots\{a-b+3\}\{a-b+1\}, \quad (2-10)$$

where the notation  $\{y\}$  is defined as

$$\{y\} = \frac{\left(\frac{y+1}{2\lambda}\right)\left(\frac{y-1}{2\lambda}\right)}{\left(\frac{y+1}{2\lambda} - 1\right)\left(\frac{y-1}{2\lambda} + 1\right)}$$

and satisfies the relations  $\{y\}\{-y\} = 1$  and  $\{y+2\lambda\} = \{-y\}$ . The scattering amplitude of the soliton (antisoliton) and breather  $S^{(a)}(u) = S_{a+}^{a+}(u) = S_{a-}^{a-}(u)$  is given as

$$S^{(a)}(u) = \begin{cases} \{a-1+\lambda\}\{a-3+\lambda\}\dots\{1+\lambda\} & \text{if } a \text{ is even} \\ -\{a-1+\lambda\}\{a-3+\lambda\}\dots\{2+\lambda\}\left(\frac{\lambda+1}{2\lambda}\right)\left(\frac{\lambda-1}{2\lambda}\right) & \text{if } a \text{ is odd} \end{cases} \quad (2-11)$$

Demanding the wave function periodic in  $L$  we have the constraints between hole densities with particle densities. For soliton states  $(n_0, n_d, n_{h0})$  we have

$$\exp(iLM_0 \sinh \theta_i^0) \prod_{j=1, \neq i}^N \left\{ S_{00}(\theta_i^0 - \theta_j^0) S_{00}(\theta_i^0 + \theta_j^0) S_{00}(2\theta_i^0) S_{0d}(\theta_i^0 - \theta_j^d) S_{0d}(\theta_i^0 + \theta_j^d) \right. \\ \left. \prod_{a=1}^{n_b} \left( S_{0a}(\theta_i^0 - \theta_j^a) S_{0a}(\theta_i^0 + \theta_j^a) \right) \right\} = \pm e^{2\pi i(n_0(\theta_i^0) + n_d(\theta_i^0) + n_{h0}(\theta_i^0))}. \quad (2-12)$$

For breathers  $(n_a, n_{ah}, a = 1, 2, \dots, n_b)$ :

$$\exp(iLM_a \sinh \theta_i^a) \prod_{j=1, \neq i}^N \left\{ S_{aa}(\theta_i^a - \theta_j^a) S_{aa}(\theta_i^a + \theta_j^a) S_{aa}(2\theta_i^a) S_{a0}(\theta_i^a - \theta_j^0) S_{a0}(\theta_i^a + \theta_j^0) \right. \\ \left. S_{ad}(\theta_i^a - \theta_j^d) S_{ad}(\theta_i^a + \theta_j^d) \prod_{b=1}^n \left( S_{ab}(\theta_i^a - \theta_j^b) S_{ab}(\theta_i^a + \theta_j^b) \right) \right\} \\ = \pm e^{2\pi i(n_a(\theta_i^a) + n_{ha}(\theta_i^a))}. \quad (2-13)$$

Differentiating with respect to the rapidity, we have the relations of hole and particle spectral densities:

$$M_A \cosh \theta + \sum_{B=0,1,\dots,n_b} \int_0^{\infty} d\theta^B \rho_B(\theta^B) (\phi_{AB}(\theta^A - \theta^B) + \phi_{AB}(\theta^A + \theta^B)) \\ + \int_0^{\infty} d\theta^d \rho_d(\theta^d) (\phi_{Ad}(\theta^A - \theta^d) + \phi_{Ad}(\theta^A + \theta^d)) \\ = 2\pi(\rho_A(\theta) + \rho_{hA}(\theta) + \delta_{A0} \rho_d(\theta)) \quad \text{for } A = 0, 1, \dots, n_b, d, \quad (2-14)$$

where  $\rho_A(\theta) = \frac{1}{L} \frac{dn_A(\theta)}{d\theta}$ ,  $\phi_{AB}(\theta) = -i \frac{d \ln S_{AB}(\theta)}{d\theta}$  and  $\phi_{Ad}(\theta) = 2\phi_{A0}(\theta)$ .

Introducing pseudo energies,  $\epsilon$

$$e^{-\epsilon_a} = \frac{\rho_a}{\rho_{ha}} \quad \text{for } a = 1, \dots, n_b, \quad e^{-\epsilon_0} = \frac{\rho_0}{\rho_{h0}}, \quad e^{-\epsilon_d} = \frac{\rho_d}{\rho_{h0}},$$

and minimizing  $f_{\alpha\beta}(R)$  we have the massive TBA:

$$\begin{aligned} \epsilon_A(\theta) &= d_A(\theta) - \ln \lambda_{\alpha\beta}^A - \frac{1}{2\pi} \sum_{B=0,1,\dots,n_b} \int_{-\infty}^{\infty} d\theta' \phi_{AB}(\theta - \theta') L_B(\theta'), \\ \epsilon_d(\theta) &= 2(\epsilon_0 + \ln \lambda_{\alpha\beta}^0) - \ln \lambda_{\alpha\beta}^d, \end{aligned} \quad (2-15)$$

where  $d_A(\theta) = 2M_A R \cosh \theta$ ,  $L_0 = \ln(1 + e^{-\epsilon_0} + e^{-\epsilon_d})$ , and  $L_a = \ln(1 + e^{-\epsilon_a})$  ( $a = 1, \dots, n_b$ ).

Shifting the pseudo energy  $\epsilon_A \rightarrow \epsilon_A - \ln \lambda_A$ , we have  $\epsilon_d = 2\epsilon_0$  and the boundary TBA is put equivalently as

$$\epsilon_A(\theta) = d_A(\theta) - \frac{1}{2\pi} \sum_B \int_{-\infty}^{\infty} d\theta' \phi_{AB}(\theta - \theta') \widetilde{L}_B(\theta') \quad (2-16)$$

where  $A = 0, 1, \dots, n_b$  and

$$\begin{aligned} \widetilde{L}_0 &\equiv \ln(1 + \lambda_{\alpha\beta}^0 e^{-\epsilon_0} + \lambda_{\alpha\beta}^d e^{-2\epsilon_0}) \\ \widetilde{L}_a &\equiv \ln(1 + \lambda_{\alpha\beta}^a e^{-\epsilon_a}) \quad \text{for } a = 1, \dots, n_b. \end{aligned}$$

In terms of this TBA, the free energy has the form,

$$E(R) = R f(R) = R \mathcal{E}_{\text{bulk}} + \mathcal{E}_{\text{boundary}} - \frac{\pi}{24R} c_{\text{eff}} \quad (2-17)$$

where  $\mathcal{E}_{\text{bulk}} = -\frac{1}{4} M^2 \tan \frac{\pi}{2\lambda}$  is the bulk energy density,  $\mathcal{E}_{\text{boundary}}$  is the boundary energy obtained by Al. Zamolodchikov [16], whose details can be found in [17]

$$\mathcal{E}_{\text{boundary}}(\eta, \vartheta) = -\frac{M}{2 \cos(\pi/2\lambda)} \left( \cos\left(\frac{\eta}{\lambda}\right) + \cosh\left(\frac{\vartheta}{\lambda}\right) - \frac{1}{2} \cos\left(\frac{\pi}{2\lambda}\right) + \frac{1}{2} \sin\left(\frac{\pi}{2\lambda}\right) - \frac{1}{2} \right),$$

and  $c_{\text{eff}}$  is the effective central charge

$$c_{\text{eff}}(RM) = \frac{6RM}{\pi^2} \int_{-\infty}^{\infty} d\theta \sum_{A=0,1,\dots,n_b} m_A \cosh \theta \widetilde{L}_A(\theta).$$

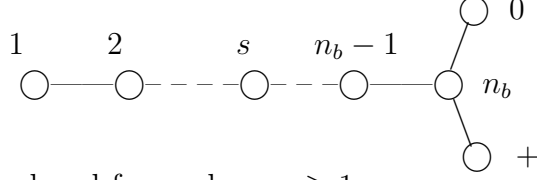
One may also put this TBA in a reduced form as in a bulk TBA [18] for  $n_b \geq 1$ . To do this, we include the doublet formally by extending the whole index into  $A' = 0, 1, \dots, n_b, +$

$$\epsilon_{A'}(\theta) = d_{A'}(\theta) - \frac{1}{2\pi} \sum_{B'=0,1,\dots,n_b,+} \int_{-\infty}^{\infty} d\theta' \phi_{A'B'}(\theta - \theta') \widetilde{L}_{B'}(\theta') \quad (2-18)$$

where  $+$  denotes the doublet,  $\epsilon_+ \equiv \epsilon_d/2$ ,  $m_+ \equiv m_0$ , and  $\widetilde{L}_+ \equiv 0$ . Then using an identity of the fourier transformed form of the kernel,  $\widetilde{\varphi}_{A'B'}(k) = \int_{-\infty}^{\infty} d\theta \phi_{A'B'}(\theta) e^{ik\theta}$ ,

$$\left( \delta_{A'B'} - \frac{1}{2\pi} \widetilde{\varphi}_{A'B'}(k) \right)^{-1} = \delta_{A'B'} - \frac{1}{2 \cosh(k\pi/h)} \mathcal{I}_{A'B'} \quad (2-19)$$

where  $h = 2\lambda = 2n_b + 2$  and  $\mathcal{I}_{A'B'}$  is the incidence matrix of  $D_{n_b+2}$ , [4, 18, 19] ( $\mathcal{I}_{A'B'} = 1$  if  $A'B'$  is directly connected, 0 otherwise),



we can put the TBA in a reduced form when  $n_b \geq 1$ ,

$$\epsilon_{A'}(\theta) = d_{A'}(\theta) + \sum_{B'=0,1,\dots,n_b,+} \mathcal{I}_{A'B'} \int_{-\infty}^{\infty} d\theta' K(\theta - \theta') (\widetilde{L}_{B'} + \epsilon_{B'} - d_{B'}) (\theta'), \quad (2-20)$$

where  $K(\theta)$  is the reduced kernel,

$$K(\theta) = \frac{\lambda}{2\pi \cosh(\lambda \theta)}$$

This reduced TBA allows one to construct Y-system equations with  $Y(\theta) = e^{\epsilon(\theta)}$ ,

$$\begin{aligned} Y_0(\theta + \frac{i\pi}{h}) Y_0(\theta - \frac{i\pi}{h}) &= [\lambda_{n_b}(\theta) + Y_{n_b}(\theta)] \\ Y_{n_b}(\theta + \frac{i\pi}{h}) Y_{n_b}(\theta - \frac{i\pi}{h}) &= [\lambda_d(\theta) + \lambda_0(\theta) Y_0(\theta) + Y_0(\theta)^2] [\lambda_{n_b-1}(\theta) + Y_{n_b-1}(\theta)] \\ Y_a(\theta + \frac{i\pi}{h}) Y_a(\theta - \frac{i\pi}{h}) &= \prod_b [\lambda_b(\theta) + Y_b(\theta)]^{\mathcal{I}_{ab}} \quad \text{for } a = 1, 2, \dots, n_b - 1 \\ Y_+(\theta) &= Y_0(\theta). \end{aligned} \quad (2-21)$$

### 3 Massless TBA for boundary sine-Gordon model

The massive TBA shows the scale dependence as well as the parametric dependence. Since we are particularly interested in the parametric dependence of the boundary TBA on  $\phi_0$ , we will look at the massless limit of the TBA in this paper.

The massless TBA corresponding to bSG action Eq. (1-1) is obtained by taking the limit  $\mu \rightarrow 0$  of the massive TBA in Eq. (2-16, 2-20). Even though the soliton mass  $M$  vanishes, one may introduce a finite renormalized mass scale  $M_R$  as  $M_R = (M/2)e^{\theta_0}$  if a large parameter  $\theta_0$  is defined as

$$e^{-\theta_0} = (C_0 \mu)^{\frac{\lambda+1}{2\lambda}} / M_R, \quad C_0 = \frac{\pi}{\gamma(b^2)} \left( \frac{\Gamma(\frac{b^2}{2-2b^2})}{\sqrt{\pi} \Gamma(\frac{1}{2-2b^2})} \right)^{2\lambda/(\lambda+1)}.$$

In this limit, the rapidity is rescaled into renormalized one,  $\theta_R$  as  $\theta = \theta_R + \theta_0$ . The boundary scattering parameter,  $\vartheta$  is also rescaled as  $\vartheta_R$  maintaining a relation  $\vartheta - \lambda\theta = \vartheta_R - \lambda\theta_R$ . Then  $\vartheta_R$  is written in terms of the action parameters,

$$(m_R)^{b^2\lambda} e^{b^2\vartheta_R} = 2\mu_B \sqrt{C_0 \sin(b^2\pi)}. \quad (3-1)$$



On the other hand,  $\eta$  is not rescaled but is identified as

$$b^2\eta = \begin{cases} b\phi_0 & \text{for } 0 \leq b\phi_0 \leq \pi/2, \\ \pi - b\phi_0 & \text{for } \pi/2 \leq b\phi_0 \leq \pi. \end{cases} \quad (3-2)$$

This identification is justified from the numerical analysis later on. In terms of this rescaled parameter (we omit hereafter the subscript  $R$  standing for the renormalized one) the solitonic boundary scattering amplitudes are given as

$$K(\eta, \vartheta, u) \rightarrow \begin{pmatrix} e^{-i\eta} e^{\frac{1}{2}(\vartheta+i\lambda\tilde{u})} & -ie^{-\frac{1}{2}(\vartheta+i\lambda\tilde{u})} \\ -ie^{-\frac{1}{2}(\vartheta+i\lambda\tilde{u})} & e^{i\eta} e^{\frac{1}{2}(\vartheta+i\lambda\tilde{u})} \end{pmatrix} e^{-i3\pi\lambda/4} k(u) \quad (3-3)$$

where  $\tilde{u} = \pi/2 - u$  and  $k(u)^{-1} = \prod_{q=0}^{n_b} 2 \cos\left(\frac{\pi}{2\lambda}\left(\frac{1}{2} + q + \frac{i\vartheta - \lambda\tilde{u}}{\pi}\right)\right)$ , and the breather boundary reflection amplitudes are given as

$$K^{(k)}(\vartheta, \eta, u) \rightarrow \prod_{l=0}^{k-1} \frac{\sin\left(\frac{1}{2}\left(\tilde{u} - \frac{i\vartheta}{\lambda} - \frac{\pi}{2} - \pi \frac{k-2l-1}{2\lambda}\right)\right)}{\sin\left(\frac{1}{2}\left(\tilde{u} - \frac{i\vartheta}{\lambda} + \frac{\pi}{2} - \pi \frac{k-2l-1}{2\lambda}\right)\right)} \quad (3-4)$$

The boundary  $\lambda_{\alpha\beta}$  is given as

$$\begin{aligned} \lambda_{\alpha\beta}^0 &= 2 \left\{ \cos \eta e^{\left(\frac{\vartheta_\alpha + \vartheta_\beta}{2} - \lambda\theta\right)} + e^{-\left(\frac{\vartheta_\alpha + \vartheta_\beta}{2} - \lambda\theta\right)} \right\} \overline{k_\alpha(u)} k_\beta(u), \\ \lambda_{\alpha\beta}^d &= \left\{ e^{(\vartheta_\alpha - \lambda\theta - i\pi\lambda/2)} + e^{-(\vartheta_\alpha - \lambda\theta - i\pi\lambda/2)} \right\} \\ &\quad \left\{ e^{(\vartheta_\beta - \lambda\theta + i\pi\lambda/2)} + e^{-(\vartheta_\beta - \lambda\theta + i\pi\lambda/2)} \right\} \left( \overline{k_\alpha(u)} k_\beta(u) \right)^2 \end{aligned} \quad (3-5)$$

From this massless scattering data the massless TBA is given as the form

$$\epsilon_A(\theta) = D_A(\theta) - \frac{1}{2\pi} \sum_B \int_{-\infty}^{\infty} d\theta' \phi_{AB}(\theta - \theta') \widetilde{L}_B(\theta') \quad (3-6)$$

where  $D_{A'} = 2m_{A'} r e^\theta$  with  $r = MR$  and the soliton mass  $M$  in  $M_{A'}$  is replaced by the renormalized mass  $M_R$ . The reduced form of TBA can be similarly obtained. TBA Eq. (3-6), however, turns out to be better suited for the numerical analysis of various range of parameters. The free energy is given as

$$R f(R) = \mathcal{E}_{\text{boundary}} - \frac{\pi}{24R} c_{\text{eff}} \quad (3-7)$$

where the bulk energy density vanishes, and the boundary energy and effective central charge are given as

$$\begin{aligned} \mathcal{E}_{\text{boundary}} &= -\frac{M}{2 \cos(\pi/2\lambda)} e^{\vartheta/\lambda} \\ c_{\text{eff}} &= \frac{12r}{\pi^2} \int_{-\infty}^{\infty} d\theta \sum_{A=0,1,\dots,n_b} m_A e^\theta \widetilde{L}_A(\theta). \end{aligned}$$

Let us investigate the parametric dependence of the ground state energy Eq. (3-7) using TBA Eq. (3-6). For the details of analysis, we will restrict our selves to  $\lambda = 1$  and  $\lambda = 2$  cases with the symmetric boundaries ( $\vartheta_\alpha = \vartheta_\beta = \vartheta$ ).

When  $\lambda = 1$  ( $n_b = 0$ ), the boundary contribution is given explicitly as,

$$\lambda_{\alpha\beta}^0 = \frac{2 \left[ \cos \eta e^{\left(\frac{\vartheta_\alpha + \vartheta_\beta}{2} - \theta\right)} + e^{-\left(\frac{\vartheta_\alpha + \vartheta_\beta}{2} - \theta\right)} \right]}{4 \cosh\left(\frac{\vartheta_\alpha - \theta}{2}\right) \cosh\left(\frac{\vartheta_\beta - \theta}{2}\right)}, \quad \lambda_{\alpha\beta}^d = \tanh\left(\frac{\vartheta_\alpha - \theta}{2}\right) \tanh\left(\frac{\vartheta_\beta - \theta}{2}\right).$$

TBA is trivial since the kernel  $\phi(\theta) = 0$ :  $\epsilon_0(\theta) = 2m_0 r e^\theta$ . The effective central charge is obtained numerically and is plotted  $c_{\text{eff}}$  v.s.  $\chi$  in Fig. 4 where  $\chi = b(\phi_0^{(2)} - \phi_0^{(1)})$ . (One may put  $\phi_0^{(1)} = 0$  using the freedom of field translation). We note that  $c_{\text{eff}}$  is  $\pi$ -periodic in  $\chi$ . This is because the boundary fugacity  $\lambda_{\alpha\beta}^0$  in Eq. (3-5) is  $2\pi$ -periodic in  $\eta = \eta_1 - \eta_2$  and  $\lambda_{\alpha\beta}$  is  $\eta$  independent. Generally,  $c_{\text{eff}}$  will be  $2\pi b^2$ - periodic in  $\chi$ .

However, the periodicity of the energy in  $\chi$  is not acceptable as pointed out in [2]. When  $\chi > \pi/2$ , the boundary term in the Lagrangian effectively changes the relative sign; one can equivalently put  $\mu_B^{(1)} \rightarrow -\mu_B^{(1)}$  and  $\mu_B^{(2)} \rightarrow \mu_B^{(2)}$  while  $\chi \rightarrow \pi - \chi$ . This relative sign change of the boundary term should be reflected in the  $c_{\text{eff}}$  value. The same problem was also observed in boundary Lee-Yang model [13].

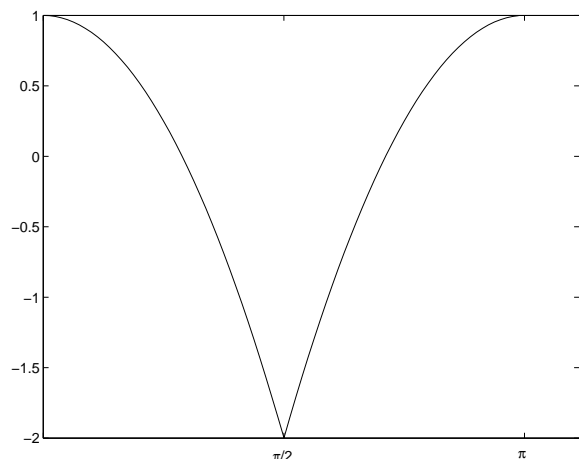


Figure 4:  $c_{\text{eff}}$  vs.  $\chi$  when  $\lambda = 1$  and  $\vartheta = 10$  before modifying the massless TBA.

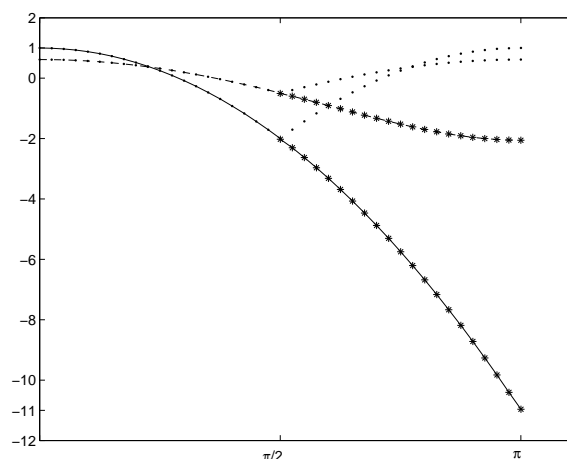


Figure 5:  $c_{\text{eff}}$  vs.  $\chi$  when  $\lambda = 1$ . Modified TBA shows the correct behavior (in stars) for  $\vartheta = 10$  (sold) and  $\vartheta = 0$  (dashed).

To cure this disease it has been proposed in [2, 13] that a certain excited state contribution should be properly taken care of. According to this proposal, the  $c_{\text{eff}}$  is recalculated and is presented in Fig. 5 when  $\lambda = 1$ . In the analysis two things are considered for  $\chi > \pi/2$ : First, one needs to find the zeroes of  $e^{\tilde{L}_0}$  in terms of the complex rapidity  $\tilde{\theta}$  following [11] with the parameter identification in Eq. (3-2).

$$1 + \lambda_{\alpha\beta}^0 e^{-\epsilon_0(\tilde{\theta})} + \lambda_{\alpha\beta}^d e^{-2\epsilon_0(\tilde{\theta})} = 0. \quad (3-8)$$

Eq. (3-8) is solved numerically. It turns out that there are infinite number of solutions for  $\tilde{\theta} = \pm i\pi/2 + \theta_p$  with  $\theta_p$  real and therefore, the pseudo energy is given as  $\epsilon_0(\tilde{\theta}) = \pm i2m_0 r e^{\theta_p}$ .

Second, one needs to take account this branch singularity effect into the free energy. To understand which solution has the effect on the free energy for  $\chi > \pi/2$ , we just complexify

the value of  $\chi$  (equivalently  $\phi_0$ ) around  $\pi/2$  (cusp point) as  $\chi \rightarrow \pi/2 - (\frac{\pi}{20})e^{i\pi k}$  with  $k$  varying from  $0 \rightarrow 1$  and use the TBA Eq. (3-6) allowing  $\theta$  complex but  $\theta'$  real to trace the movement of singularities. With the notation  $t_0 \equiv e^{\tilde{L}_0} = 1 + \lambda_{\alpha\beta}^0 e^{-\epsilon_0} + \lambda_{\alpha\beta}^d e^{-2\epsilon_0}$ , the result is given in Fig. 6 for  $\vartheta =$ . We choose the case of  $\vartheta = 0$  since this does not correspond to the conformal boundary condition, neither Dirichlet nor Neumann condition. (Note that the singularity position is contour plotted using  $1/(1 + |t_0|)$  rather than  $1/|t_0|$  to renormalize the height).

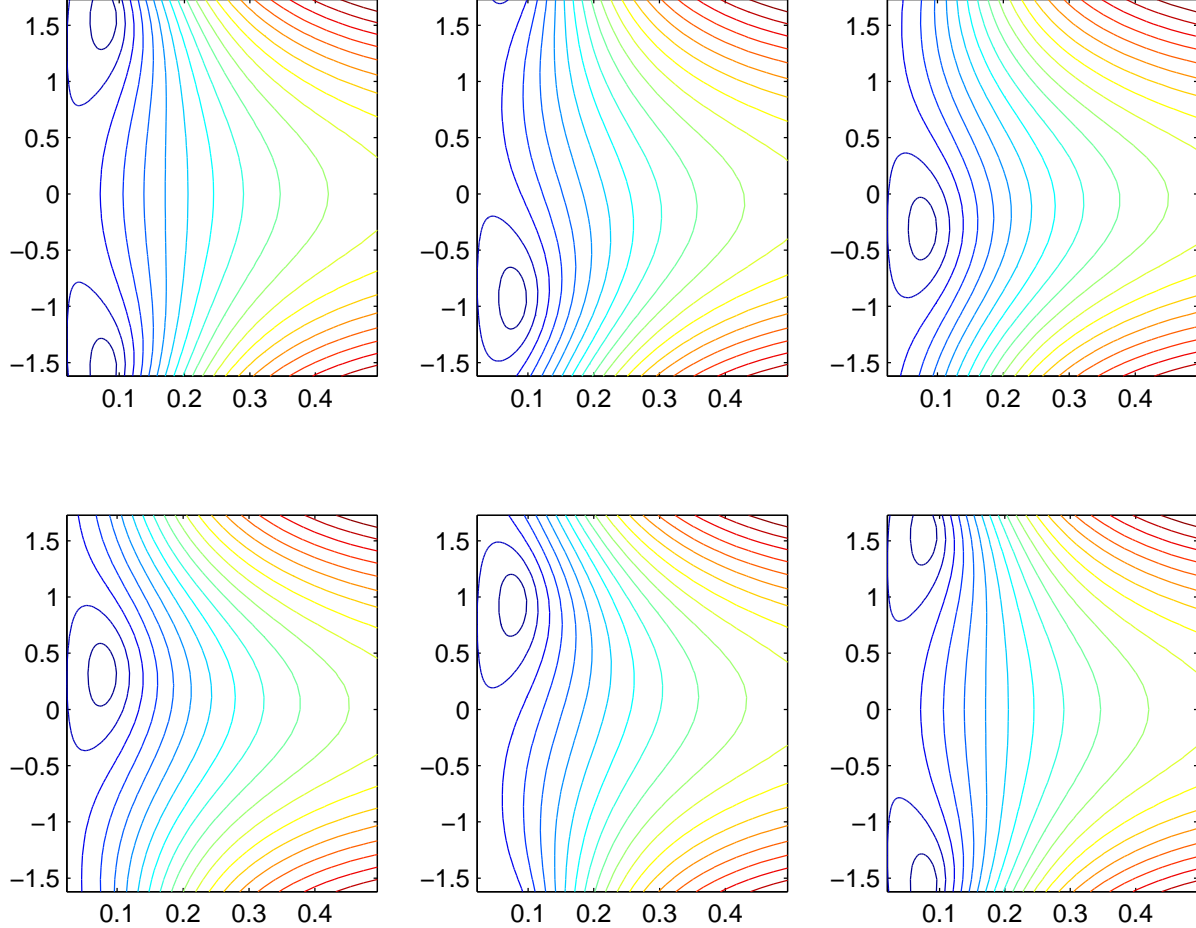


Figure 6: Singularity crossing for  $\lambda = 1$  case: Contour plot of  $1/(1 + |t_0|)$  is presented in the complex  $\theta$  plane. The vertical axis stands for  $-\frac{\pi}{2} \leq \text{Im}(\theta) \leq \frac{\pi}{2}$  and the horizontal one for  $0 < e^{\text{Re}(\theta)} < 0.5$ . From the top left to the bottom right, each figure is reproduced for  $\chi = \pi/2 - \frac{\pi}{20}e^{i\pi k}$  with  $k = 0, 1/5, 2/5, 3/5, 4/5, 1$  for  $\vartheta = 0$ .

When  $\chi = \text{real}$ , singularities lie on the imaginary value  $\text{Im}(\tilde{\theta}) = \pm i\pi/2$ . Only one of the singularities (the left-most one with the smallest value of  $\theta_p$ ) crosses the real rapidity line during the complexified changes of  $\chi$  from the negative imaginary value  $-i\pi/2$  to the positive imaginary plane and finally sits at the positive imaginary value  $i\pi/2$ . (When  $k$  varies from 0 to  $-1$ , the left-most singularity at  $i\pi/2$  is moving down and crosses the real axis). The other singularities remains in the imaginary axis with  $\text{Im}(\theta) = \pm\pi/2$ . This is seen in Fig. 7. Similar behavior is demonstrated in scaling Lee-Yang model [11, 12, 14]

and used in boundary SLYM [13]. (Crossing singularities are paired for massive theories).

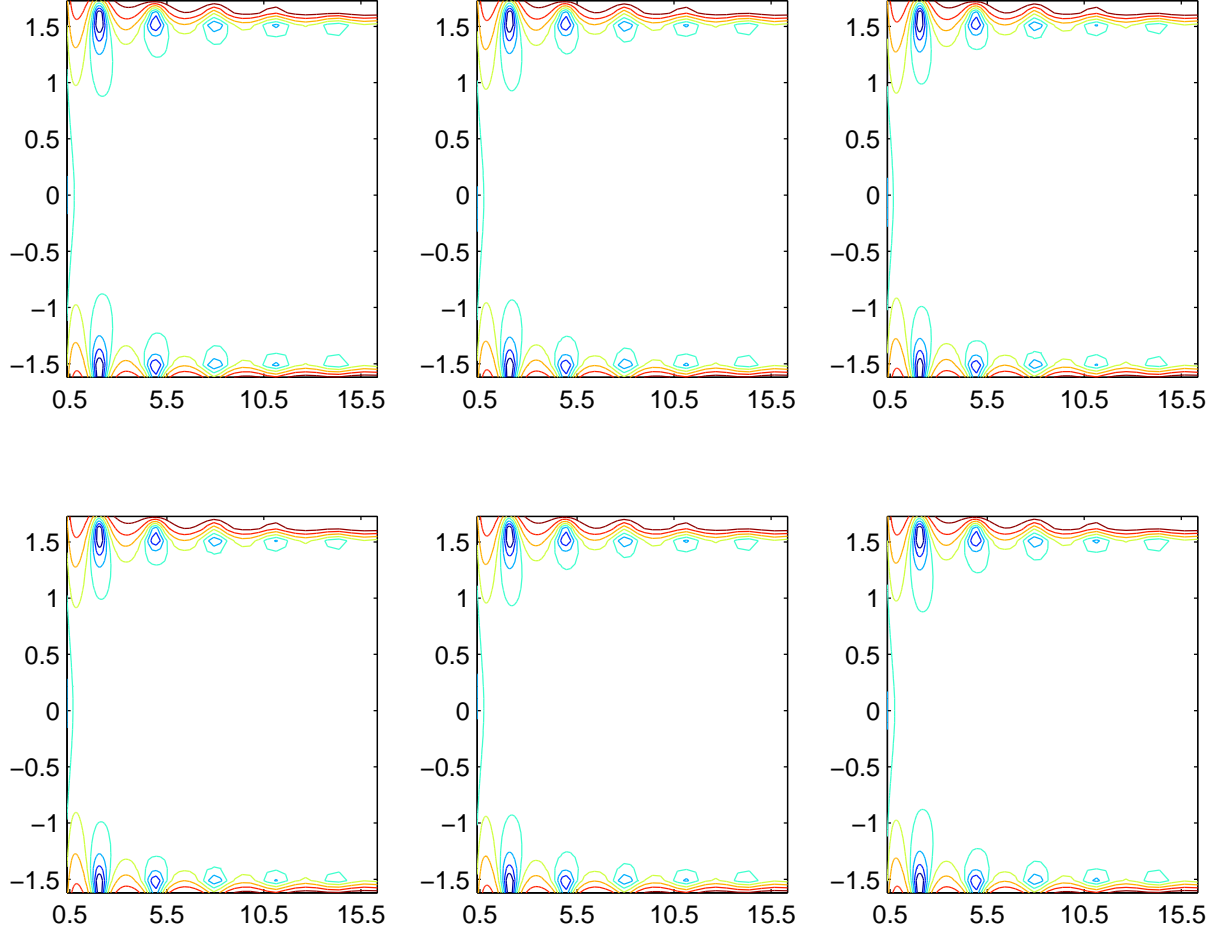


Figure 7: Other singularities for  $\lambda = 1$  case: Contour plot of  $1/(1 + |t_0|)$  is presented in the complex  $\theta$  plane. The vertical axis stands for  $-\frac{\pi}{2} \leq \text{Im}(\theta) \leq \frac{\pi}{2}$  and the horizontal for  $0.5 \leq e^{\text{Re}(\theta)} \leq 16$ . From the top left to the bottom right, each figure is reproduced for  $\chi = \pi/2 - \frac{\pi}{20}e^{i\pi k}$  with  $k = 0, 1/5, 2/5, 3/5, 4/5, 1$  for  $\vartheta = 0$ .

Due to this singularity crossing, the rapidity integration in the free energy has to detour the branch singularity. As the singularity crosses the real axis and moves up to  $\text{Im}(\tilde{\theta}) = \pi/2$  and one has to evaluate the contour integration around the singularity  $\tilde{\theta} = i\pi/2 + \theta_p$ . The result is given as

$$-\frac{\pi}{24r}c_{\text{eff}} = -im_0 e^{\tilde{\theta}} - \frac{1}{2\pi} \int_{-\infty}^{\infty} d\theta m_0 e^{\theta} \tilde{L}_0(\theta), \quad (3-9)$$

where  $\int$  represents the principal value of the integration. The the first term in the RHS is the singularity crossing contribution and the second one is the real axis contribution. (Here we adopt the convention of the singularity crossing from the negative imaginary value to the positive imaginary one. One may equivalently consider the opposite singularity crossing and detour the integration to the negative imaginary complex plane and get the same result. Note that if  $\tilde{\theta}$  is a solution, so is  $\tilde{\theta}^*$ ).

We generalize this idea into the case  $\lambda > 1$ . To understand the singularity crossing, we need to know the singularity structure in the complex  $\theta$  plane. Note that the TBA Eq. (3-6) is singularity-free on the rapidity domain with  $-\pi/h < \text{Im}(\theta) < \pi/h$  when  $\chi$  is real. One can analytically continue the TBA into other domain of  $\theta$  using the relation of Y-system Eq. (2-21).

When  $\lambda = 2$  the boundary  $\lambda_{\alpha\beta}$  is given as

$$\begin{aligned}\lambda_{\alpha\beta}^0 &= \frac{2 \left[ \cos \eta e^{\left(\frac{\vartheta_\alpha + \vartheta_\beta}{2} - 2\theta\right)} + e^{-\left(\frac{\vartheta_\alpha + \vartheta_\beta}{2} - 2\theta\right)} \right]}{\left[ 4 \cosh\left(\frac{\vartheta_\alpha - 2\theta}{4} + \frac{i\pi}{8}\right) \cosh\left(\frac{\vartheta_\alpha - 2\theta}{4} - \frac{i\pi}{8}\right) \right] \left[ 4 \cosh\left(\frac{\vartheta_\beta - 2\theta}{4} + \frac{i\pi}{8}\right) \cosh\left(\frac{\vartheta_\beta - 2\theta}{4} - \frac{i\pi}{8}\right) \right]}, \\ \lambda_{\alpha\beta}^d &= \frac{4 \cosh(\vartheta_\alpha - 2\theta) \cosh(\vartheta_\beta - 2\theta)}{\left( 4 \cosh\left(\frac{\vartheta_\alpha - 2\theta}{4} + \frac{i\pi}{8}\right) \cosh\left(\frac{\vartheta_\alpha - 2\theta}{4} - \frac{i\pi}{8}\right) \right)^2 \left( 4 \cosh\left(\frac{\vartheta_\beta - 2\theta}{4} + \frac{i\pi}{8}\right) \cosh\left(\frac{\vartheta_\beta - 2\theta}{4} - \frac{i\pi}{8}\right) \right)^2}, \\ \lambda_{\alpha\beta}^1 &= \tanh(\theta/2 - \vartheta_\alpha/4) \tanh(\theta/2 - \vartheta_\beta/4),\end{aligned}\tag{3-10}$$

where  $\eta$  parameter is identified according to Eq. (3-2) and the kernel is given as

$$\phi_{00}(\theta) = \frac{1}{2}\phi_{11}(\theta) = -\frac{1}{\cosh \theta}, \quad \phi_{01}(\theta) = -\frac{2\sqrt{2} \cosh(\theta)}{\cosh(2\theta)}.$$

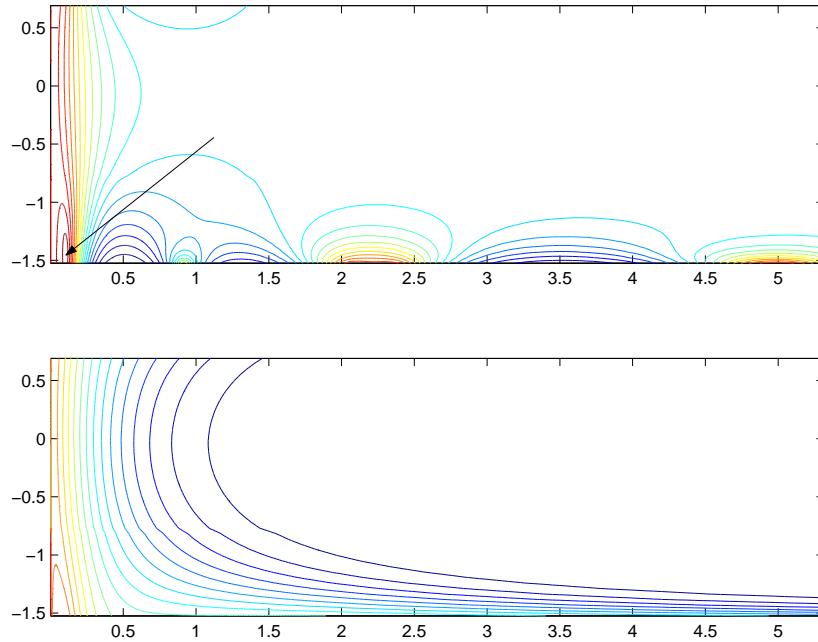


Figure 8: Singularity structure of TBA in the complex  $\theta$  plane when  $\lambda = 2$  and  $\chi = \pi/3 - \pi/30$ : Contour plot of  $1/(1 + |t_0|)$  (up) and  $1/(1 + |z_1|)$  (down). The vertical axis stands for  $-\frac{\pi}{2} \leq \text{Im}(\theta) \leq \frac{\pi}{4}$  and the horizontal one for  $0 \leq e^{\text{Re}(\theta)} \leq 6$ . The  $t_0$  zero with the arrow attached is moving.

$c_{\text{eff}}$  is  $\pi$ -periodic in  $\chi$  and has the cusp at  $\pi/3$ . (See Fig. 14 below). Fig. 8 is the numerical study of the singularity in the domain with  $\text{Im}(\theta) \leq \pi/2$  at real  $\chi = \pi/3 - \pi/30$

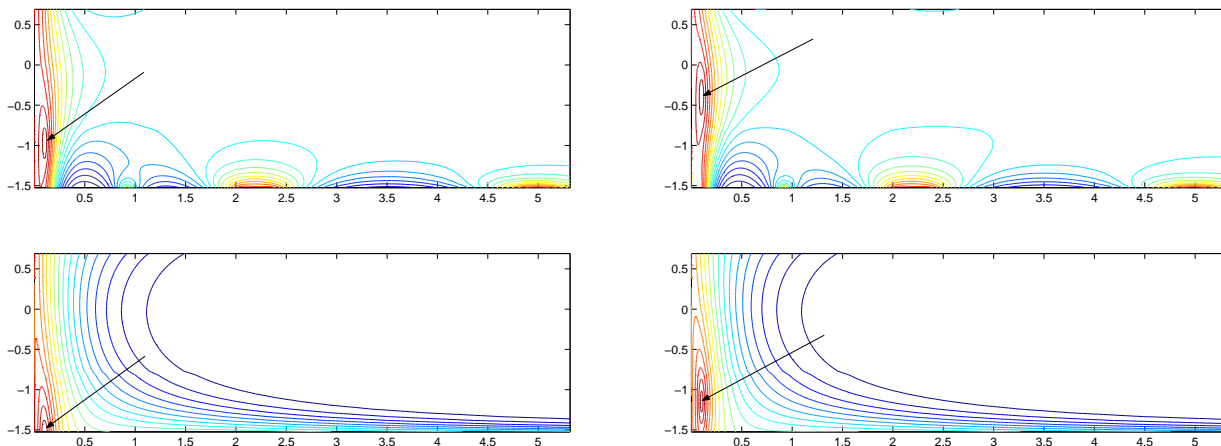


Figure 9: Contour plot of  $1/(1+|t_0|)$  (up) and  $1/(1+|z_1|)$  (down) for  $k = 0.25$  (left) and  $k = 0.5$  (right). The vertical axis stands for  $-\frac{\pi}{2} \leq \text{Im}(\theta) \leq \frac{\pi}{4}$  and the horizontal one for  $0 \leq e^{\text{Re}(\theta)} \leq 6$ . The moving zeros of  $t_0$  and  $z_1$  are pointed with arrows.

below the cusp point. Here  $t_0 \equiv e^{\tilde{L}_0}$ . In the figure  $z_1 \equiv e^{\epsilon_1}$  and  $1/(1+|t_0|)$  and  $1/(1+|z_1|)$  are plotted after normalizing  $1/|t_0|$  and  $1/|z_1|$ .

It is to noted that all the zeros of  $t_0$  lie at  $\text{Im}(\theta) = \pm\pi/2$  instead of  $\text{Im}(\theta) = \pm\pi/4$ . In addition, there are no zeros of  $z_1$  in this domain. (Note that pseudo energy  $\epsilon_A$  is symmetric under  $\theta \rightarrow \theta^*$  when  $\chi$  is real).

Next, the singularity positions are traced with the complexified  $\chi$ .  $\chi$  is put as  $\chi \rightarrow \frac{\pi}{3} - (\frac{\pi}{30})e^{i\pi k}$  and  $k$  is varied  $0 \rightarrow 1$ . The numerical result is given in Fig. 9. As  $k$  increases, one of the  $t_0$  zeros (with the smallest value of real rapidity) goes up. When  $k = 0.25$ , one zero of  $z_1$  with the same real rapidity appears at  $\text{Im}(\theta) = -\pi/2$  and moves up as  $k$  increases. As  $k$  reaches 0.5, the zero of  $z_1$  comes to  $\text{Im}(\theta) = -\pi/4$ .

In fact the positions of zeros of each species are related with the positions of zeros of other species according to the Y-system Eq. (2-21). As the singularity of one species moves around, the corresponding singularities of other species follow the trace.

The position of  $t_0$  zero is drawn in Figs. (10, 11). The data is taken up to  $k = 0.5$  without any difficulty. However, beyond  $k = 0.5$  numerical work becomes harder due to the numerical instability. We use the method using the “damped” iterative method used in [11] to easy this instability up to near  $k = 0.56$ . Beyond that point numerical instability does not allow any further computation. Nevertheless, the data clearly indicates that the imaginary position changes linearly in  $k$ .

Now, it should be noted that as the  $t_0$  zero crosses the real rapidity line, we cannot use the TBA Eq. (3-6) any longer. This is because the moving singularity pushes up the real integration line of the convolution and forces to modify the TBA. Denoting the position of the  $t_0$  zero as  $\tilde{\theta}$ , we have

$$\epsilon_A(\theta) = 2m_A r e^\theta + \ln S_{A0}(\theta - \tilde{\theta}) - \frac{1}{2\pi} \sum_{B=0,1} \int_{-\infty}^{\infty} d\theta' \phi_{AB}(\theta - \theta') \tilde{L}_B(\theta'). \quad (3-11)$$

Here the branch-cut contribution is used as follows.

$$-\frac{1}{2\pi} \int d\theta' \phi_{A0}(\theta - \theta') \tilde{L}(\theta') \rightarrow \ln S_{A0}(\theta - \tilde{\theta}) - \frac{1}{2\pi} \int d\theta' \phi_{A0}(\theta - \theta') \tilde{L}(\theta').$$

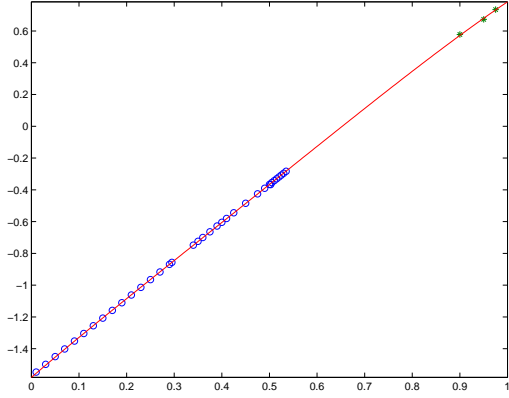


Figure 10:  $t_0$  crossing singularity position:  $e^{\text{Re}(\theta)}$  v.s.  $k$ . Data (denoted as o) for less than  $k = 0.6$  are taken from the original TBA. Data (denoted as \*) for close to  $k = 1$  are taken from the modified TBA.

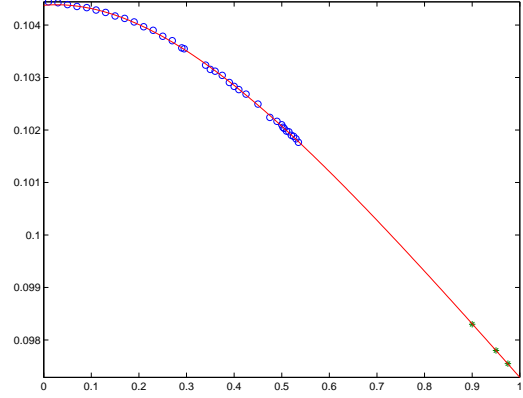


Figure 11:  $t_0$  crossing singularity position:  $\text{Im}(\theta)$  v.s.  $k$ . Data (denoted as o) for less than  $k = 0.6$  are taken from the original TBA. Data (denoted as \*) for close to  $k = 1$  are taken from the modified TBA.

Using this modified TBA Eq. (3-11) we obtain Figs. (12, 13) for the singularity structure. The figures show that  $t_0$  zero and  $z_1$  zero have the same real rapidity ( $e^{\text{Re}\theta} \approx 0.1$ ) but with the imaginary rapidity  $\pi/4$  apart. In addition, the position of  $t_0$  zero in Figs. (10, 11) (denoted as \*) ends up at the imaginary rapidity  $\pi/4$ .

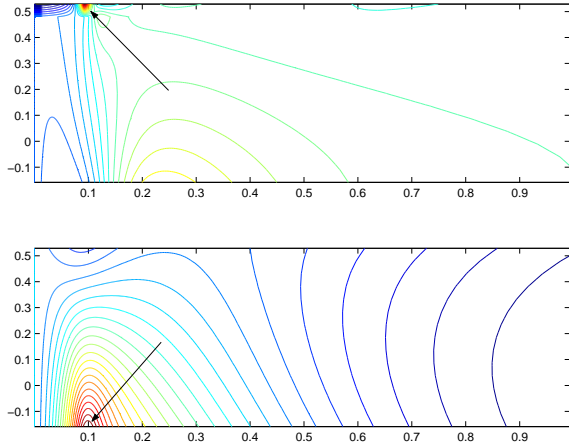


Figure 12: Position of  $t_0$  zero (up) and  $z_1$  (down) for  $k = 0.9$ . Vertical axis stands for  $0.58 - \frac{\pi}{4} \leq \text{Im}(\theta) \leq 0.58$  and horizontal one for  $0 \leq e^{\text{Re}(\theta)} \leq 1$ . The moving zeros of  $t_0$  and  $z_1$  are pointed with arrows.

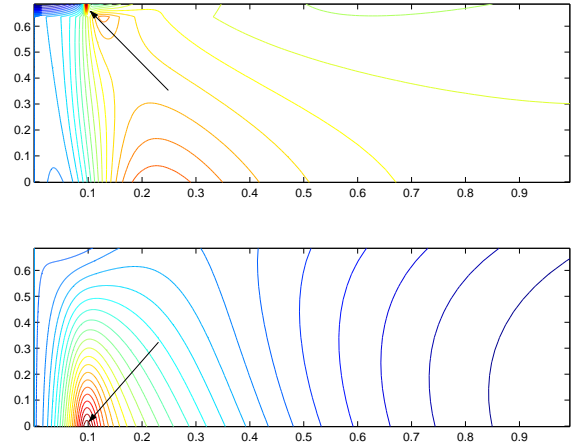


Figure 13: Position of  $t_0$  zero (up) and  $z_1$  (down) for  $k = 0.975$ . Vertical axis stands for  $0.73 - \frac{\pi}{4} \leq \text{Im}(\theta) \leq 0.73$  and horizontal one for  $0 \leq e^{\text{Re}(\theta)} \leq 1$ . The moving zeros of  $t_0$  and  $z_1$  are pointed with arrows.

As  $k$  approaches 1,  $\chi$  becomes real and the  $t_0$  zero reaches  $\text{Im}(\theta) = \pi/4$ . At the same time the zero of  $z_1$  reaches the real rapidity axis,  $\text{Im}(\theta) = 0$ . Therefore, at real  $\chi = \pi/3 + \pi/30 > \pi/3$ , the  $z_1$  zero in the convolution integration modifies TBA again.

For real  $\theta$  the pseudo energy becomes

$$\begin{aligned}\epsilon_A(\theta) &= 2m_A r e^\theta + \ln S_{A0}(\theta - \tilde{\theta}) - \frac{1}{2} \ln S_{A1}(\theta - \tilde{\theta}) - \frac{1}{2\pi} \sum_{B=0,1} \int_{-\infty}^{\infty} d\theta' \phi_{AB}(\theta - \theta') \tilde{L}_B(\theta') \\ &= 2m_A r e^\theta + \frac{1}{2} \ln \frac{S_{A0}(\theta - \tilde{\theta})}{S_{A0}(\theta - \tilde{\theta}^*)} - \frac{1}{2\pi} \sum_{B=0,1} \int_{-\infty}^{\infty} d\theta' \phi_{AB}(\theta - \theta') \tilde{L}_B(\theta').\end{aligned}\quad (3-12)$$

In the last identity the bootstrap relation of the scattering matrix is used:

$$S_{A0}(\theta - i\pi/4)S_{A0}(\theta + i\pi/4) = S_{A1}(\theta), \quad A = 1, 2.$$

Explicitly,

$$S_{00}(\theta) = i \tan\left(\frac{\theta + i\pi/2}{2}\right), \quad S_{11}(\theta) = -\left(S_{00}(\theta)\right)^2, \quad S_{10}(\theta) = \frac{1 - \sqrt{2} \cosh(\theta + i\pi/2)}{1 + \sqrt{2} \cosh(\theta + i\pi/2)}.$$

Note that the convolution integration in Eq. (3-12) refers to the principal value due to the singularity of  $\tilde{L}_1(\theta')$  at  $\theta = \theta_p$ . The numerical integration of the convolution can be done by shifting the contour integration. Another way of avoiding this numerical instability is to use TBA with the reduced kernel. Using the kernel relation (2-19), we have

$$\epsilon_{A'}(\theta) = D_{A'}(\theta) + P_{A'}(\theta) + \sum_{B'=0,1,+} \mathcal{I}_{A'B'} \int_{-\infty}^{\infty} d\theta' K(\theta - \theta') \left( \tilde{L}_{B'} + \epsilon_{B'} - D_{B'} - P_{B'} \right)(\theta') \quad (3-13)$$

where  $P_{A'}(\theta) = \frac{1}{2} \ln \frac{S_{A'0}(\theta - \tilde{\theta})}{S_{A'0}(\theta - \tilde{\theta}^*)}$  and  $D_{A'} = 2m_{A'} r e^\theta$ . Note that  $(\tilde{L}_1 + \epsilon_1)(\theta')$  vanish at  $\theta' = \theta_p$ .

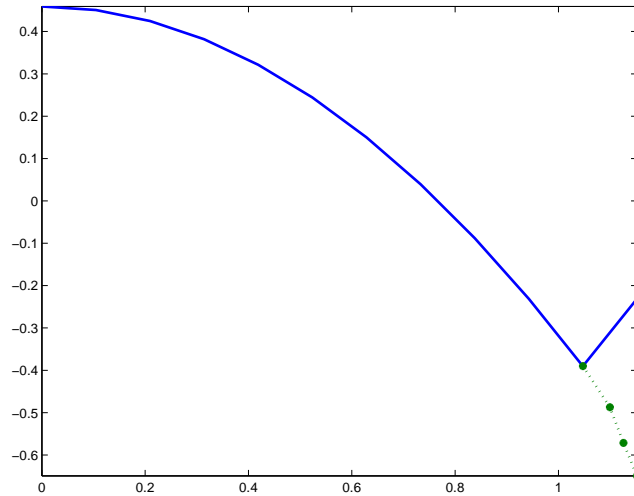


Figure 14:  $c_{\text{eff}}$  vs.  $\chi$  when  $\lambda = 2$  and  $\vartheta = 0$ : Solid line is obtained from the original TBA and dotted one from the modified TBA.

Now, the crossing singularities contribute to the free energy:

$$-\frac{\pi}{24r} c_{\text{eff}} = -\frac{m_0}{\sqrt{2}} e^{\theta_p} - \frac{1}{2\pi} \int_{-\infty}^{\infty} d\theta \sum_{A=0,1} m_A e^\theta \tilde{L}_A(\theta), \quad (3-14)$$



where  $\theta_p$  is the real part of  $\tilde{\theta}$ . This singularity position should satisfy the constraint equation,

$$t_0(\theta_p \pm i\frac{\pi}{4}) = z_1(\theta_p) = 0 \quad (3-15)$$

Thus obtained  $c_{\text{eff}}$  is compared with the original result in Fig. 14. The smooth behavior of  $c_{\text{eff}}$  in Fig. 14 indicates that the modified TBA is in the right track.

Finally, we remark that the modified TBA (3-12, 3-13) is also written in another form if the kernel relation (2-19) is used for the S-matrix:

$$\epsilon_{A'}(\theta) = D_{A'}(\theta) + \sum_{B'=0,1,+} \mathcal{I}_{A'B'} \left( \Xi(\theta, \tilde{\theta}) + \int_{-\infty}^{\infty} d\theta' K(\theta - \theta') (\widetilde{L}_{B'} + \epsilon_{B'} - D_{B'}) (\theta') \right) \quad (3-16)$$

where

$$i\Xi(\theta, \tilde{\theta}) = \tan^{-1}(\tanh(3(\theta - \tilde{\theta})/2)) - \tan^{-1}(\tanh(3(\theta - \tilde{\theta} + i\pi/2)/2)).$$

This TBA satisfies the same Y-system in Eq. (2-21) with the fugacities replaced with the massless one ( $h=4$  when  $\lambda = 2$ ). Redefining  $Y$ 's,  $y_0(\theta) = Y_0(\theta)/\sqrt{\lambda^d(\theta)}$ ,  $y_1(\theta) = Y_1(\theta)/\lambda^1(\theta)$  and  $\omega = i\pi/4$ , we may put into this form.

$$\begin{aligned} y_0(\theta + \omega) y_0(\theta - \omega) &= 1 + y_1(\theta) \\ y_1(\theta + \omega) y_1(\theta - \omega) &= 1 + \frac{\lambda^0}{\sqrt{\lambda^d}} y_0(\theta) + \left( y_0(\theta) \right)^2 \end{aligned} \quad (3-17)$$

where fugacity relations for  $\lambda = 2$  are also used,

$$\begin{aligned} \lambda_{\alpha\beta}^d(\theta + \omega) \lambda_{\alpha\beta}^d(\theta - \omega) &= \left( \lambda_{\alpha\beta}^1(\theta) \right)^2 \\ \lambda_{\alpha\beta}^1(\theta + \omega) \lambda_{\alpha\beta}^1(\theta - \omega) &= \lambda_{\alpha\beta}^d(\theta). \end{aligned}$$

Note that since  $\lambda^0(\theta)/\sqrt{\lambda^d(\theta)}$  is  $\frac{(h+2)\pi}{h} = \frac{3\pi}{2}$ -periodic in  $\theta$ , so are  $y_0(\theta)$  and  $y_1(\theta)$  as in the bulk case.

## 4 Conclusion

We presented the (R-channel) TBA for the (massless) boundary sine-Gordon theory with coupling parameter  $\lambda =$  positive integer, which incorporates the violation of the topological charge. With this TBA, the boundary parameter effect on the effective central charge is investigated.

This TBA, however, does not reflect the boundary parameter condition faithfully beyond the cusp point  $\chi = b^2\pi$ . We have demonstrated that this unpleasant feature is due to the branch singularity crossing in the TBA equation. Numerical analysis show that near the cusp point of  $c_{\text{eff}}$  some of the singularities of TBA crosses the real rapidity. It turns out that only one singularity for each species changes its position in the complex plane. Especially, its imaginary position moves “linearly” with the phase of the complexified boundary parameter  $\chi$  near the cusp. We expect this singularity crossing feature will

be very universal. When  $\lambda = 2$  ( $h = 4$  and periodicity  $\frac{3}{2}$  in unit of  $\pi$ ), the imaginary parts of the original singularity positions are  $\pm\frac{2}{4}, \pm\frac{3}{4}$ . After singularity crossing some of the positions change into  $0, \pm\frac{1}{4}$ . This leads into consideration for other  $\lambda$ 's ( $h = 2\lambda$ ). From the original singularity positions  $\pm\frac{2}{h}, \pm\frac{3}{h}, \dots, \pm\frac{\lambda}{h}, \pm\frac{\lambda+1}{h}$  with periodicity  $\frac{h+2}{h}$ , some of the singularities will presumably rearrange into  $0, \pm\frac{1}{h}, \pm\frac{2}{h}, \dots, \pm\frac{\lambda-1}{h}$ . This expectation needs to be checked further as well as the behavior for various parameter range. The scale dependence of the massive TBA is also not well understood. This issues will be carried on in a separate paper.

This analysis is also expected to hold for an arbitrary coupling constant case. However, the TBA of massless/massive boundary sine-Gordon theory with arbitrary coupling is not feasible at this moment since the bulk Hamiltonian eigenstates will result in the infinitely coupled TBA equations [20]. Instead of this approach, DDV type equation is expected to be more suitable, which does not impose the string hypothesis for the structure of the roots of Bethe ansatz [21].

It is known [22] that the sign change effect of the boundary term of boundary Liouville theory and boundary sinh-Gordon model [23] can be explained using the analytically continued boundary parameter only to a certain range. Nevertheless, the boundary Lagrangian phase difference is also known [22] to induce the branch singularity crossing similarly as in this boundary sine-Gordon model. Furthermore, the integrable boundary ADE-affine Toda theories [24] have discrete boundary conditions, (+), (-) and Neumann condition. Among the three, (-) boundary condition is not yet fully understood. It remains to be seen if there is any relation between the relative sign change of the boundary term  $\mu_B \rightarrow -\mu_B$  and the excited state contribution to  $c_{\text{eff}}$ .

*Note added:* While our manuscript being revised, a preprint by Caux et. al. (cond-mat/0306328) appeared where similar singularity structure information at the cusp point is used for the analysis of the finite size effect.

## Acknowledgement

We thank C. Ahn, P. Dorey, K. Moon and R. Tateo for invaluable discussions and KIAS for hospitality. CR thanks Al. Zamolodchikov for explaining his work on the singularity crossing in boundary sinh-Gordon model, H. Saleur for informing their singularity conjecture of TBA and Durham University where the revision of the manuscript was made. This work is supported in part by the Basic Research Program of the Korea Science and Engineering Foundation Grant number R01-1999-00018-0(2002) and by Korea Research Foundation 2002-070-C00025.

## References

- [1] P. Fendley, A. Ludwig, and H. Saleur, Phys. Rev. Lett. **74** (1995) 3005; Phys. Rev. **B 52** (1995) 8934.
- [2] J.-S. Caux, H. Saleur and F. Siano, Phys. Rev. Lett. **88** (2002) 106402.

- [3] I. Affleck, J.-S. Caux and A. M. Zagoskin, Phys. Rev. **B 62** (2000) 1433.
- [4] P. Fendley, H. Saleur, and N. P. Warner, Nucl. Phys. **B430** (1994) 577.
- [5] A. B. Zamolodchikov and Al. B. Zamolodchikov, Ann. Phys. **120** (1979) 253; L. Fadeev, E. Sklyanin and L. Takhtajan, Th. Math. Phys. **40** (1979) 688; V. E. Korepin, Th. Math. Phys. **41** (1979) 953.
- [6] A. B. Zamolodchikov, Int. J. Mod. Phys. **A4** (1989) 4235.
- [7] S. Ghoshal and A. B. Zamolodchikov, Int. J. Mod. Phys. **A9** (1994) 3841; S. Ghoshal, Int. J. Mod. Phys. **A9** (1994) 4801.
- [8] Al. B. Zamolodchikov, Nucl. Phys. **B342** (1990) 695.
- [9] C. N. Yang and C. P. Yang, J. Math. Phys. **10** (1969) 1115.
- [10] A. LeClair, G. Mussardo, H. Saleur, and S. Skorik, Nucl. Phys. **B453** (1995) 581.
- [11] P. Dorey and R. Tateo, Nucl. Phys. **B482** (1996) 639.
- [12] P. Dorey and R. Tateo, Nucl. Phys. **B515** (1998) 575.
- [13] P. Dorey, A. Pocklington, R. Tateo and G. Watts, Nucl. Phys. **B525** (1998) 641.
- [14] V. V. Bazhanov, S. L. Lukyanov, A. B. Zamolodchikov, Nucl. Phys. **B489** (1997) 487.
- [15] Al. B. Zamolodchikov, Int. J. Mod. Phys. **A10** (1995) 1125.
- [16] Al. Zamolodchikov in 5th Bologna Workshop (2001).
- [17] Z. Bajnok, L. Palla, G. Takács, Nucl. Phys. **B614** (2001) 405.
- [18] Al. B. Zamolodchikov, Phys. Lett. **B253** (1991) 391.
- [19] T. R. Klassen and E. Melzer, Nucl. Phys. **B338** (1990) 485; **B350** (1991) 635.
- [20] M. Takahashi and M. Suzuki, Prog. Th. Phys. **48** (1972) 2187.
- [21] C. Destri and H. J. de Vega, Phys. Rev. Lett. **69** (1992) 2313; Nucl. Phys. **B438** (1995) 413.
- [22] Al. Zamolodchikov, in private communication.
- [23] A. B. Zamolodchikov and Al. B. Zamolodchikov, Nucl. Phys. **B477** (1996) 577-605; V. A. Fateev, A. Zamolodchikov, and Al. Zamolodchikov, “Boundary Liouville Field Theory I. Boundary State and Boundary Two-point Function”, [hep-th/0001012](#).
- [24] E. Corrigan, P. Dorey, R. Rietdijk, and R. Sasaki, Phys. Lett. **B333** (1994) 83-91; V. Fateev, “Normalization Factors, Reflection Amplitudes and Integrable Systems”, [hep-th/0103014](#); Mod. Phys. Lett. **bf A16** (2001) 1201; C. Ahn, C. Kim, C. Rim, Nucl. Phys. **B628** (2002) 486.